Available online at www.sciencedirect.com

jmr&t Journal of Materials Research and Technology

journal homepage: www.elsevier.com/locate/jmrt

Original Article

Improved electromagnetic interference shielding performances of carbon nanotube and carbonyl iron powder (CNT@CIP)-embedded polymeric composites

Daeik Jang [a], *H.N. Yoon* [a], *Joonho Seo* [a], *Hyun Jun Cho* [b], *G.M. Kim* [c], *Young-Kwan Kim* [b,**], *Beomjoo Yang* [d,*]

[a] *Department of Civil and Environmental Engineering, Korea Advanced Institute of Science and Technology (KAIST), 291 Daehak-ro, Yuseong-gu, Daejeon 34141, Republic of Korea*

[b] *Department of Chemistry, Dongguk University-Seoul Campus, 30 Pildong-ro, Jung-gu, Seoul 04620, Republic of Korea*

[c] *Mineral Processing & Metallurgy Research Center, Resources Utilization Division, Korea Institute of Geoscience and Mineral Resources, 124 Gwahak-ro, Yuseong-gu, Daejeon 34132, Republic of Korea*

[d] *School of Civil Engineering, Chungbuk National University, 1 Chungdae-ro, Seowon-gu, Cheongju, Chungbuk 28644, Republic of Korea*

ARTICLE INFO

Article history:
Received 26 January 2022
Accepted 28 February 2022
Available online 8 March 2022

Keywords:
Carbon nanotubes (CNTs)
Carbonyl iron powder (CIP)
Electromagnetic wave
Nanohybrid

ABSTRACT

This study proposes a novel method of fabricating nanohybrid particles composed of carbon nanotubes and carbonyl iron powder (CNT@CIP), which are then embedded in a polymer for use as electromagnetic interference (EMI) shielding. First, a method of fabricating CNT@CIP nanohybrid particles is introduced, and their formation is verified using characterization tools such as zeta potential analysis, scanning electron microscopy, Fourier-transform infrared spectroscopy, and Raman spectroscopy. Then, the CNT@CIP nanohybrid particles are incorporated into a polymeric matrix. The electrical conductivity and EMI shielding capability of the resulting composites are systematically investigated. According to the experimental results, it can be found that the electrical conductivity and EMI shielding effectiveness increase with increasing of CNT@CIP nanohybrid particles contents. In addition, they are improved by the alignment of the CNT@CIP hybrid particles caused by the magnetization curing, reducing the amount of electrically conductive fillers required. Consequently, utilization of CNT@CIP nanohybrid particles and magnetization curing can greatly improve the electrical conductivity and EMI shielding capability, showing their potential as EMI shielding composites in various practical applications.

* Corresponding author.
** Corresponding author.
E-mail addresses: kimyk@dongguk.edu (Y.-K. Kim), byang@chungbuk.ac.kr (B. Yang).

https://doi.org/10.1016/j.jmrt.2022.02.134

1. Introduction

The use of electronics and 5G telecommunications technology is becoming increasingly widespread, but undesirable electromagnetic (EM) radiation can affect nearby electronics and human health [1–4]. Thus, it is necessary to develop materials for electromagnetic interference (EMI) shielding to satisfy the demands of the electronics and communications industries [5–9]. Many researchers have attempted to fabricate EMI shielding composites using carbon-based materials such as carbon nanotubes (CNTs), carbon black, and carbon fiber because they have high electrical conductivity and are excellent compatible with polymeric matrices [10–12]. Among these carbon-based materials, CNTs are considered to be a promising candidate for electrically conductive fillers in polymeric composites because they have a unique structure with a high aspect ratio. This means that high electrical conductivity can be achieved using a small amount of CNTs [13–16]. Zhao et al. [5] embedded CNTs in a sponge-type polymer, and investigated its EMI shielding capability. Their CNT-embedded sponge-type polymer provided approximately 18 dB of EMI shielding for frequencies of 8–12 GHz [5]. Nam et al. [17] produced epoxy-based polymeric composites incorporating 5 wt% of CNTs, which provided approximately 12 dB of EMI shielding for frequencies of 2–5 GHz.

Recently, carbonyl iron powder (CIP) has been highlighted for the development of EMI shielding composites due to its magnetization properties [18–20]. In particular, CIP responds to an external applied magnetic field, which means it can be controlled easily [21–23]. Chen et al. [18] fabricated epoxy nanocomposites with 30 wt% of CIP for efficient EMI shielding, and achieved 36 dB of EMI shielding for frequencies of 9.5–1.2 GHz. Wang et al. [19] fabricated 70 wt% CIP-embedded polymeric composites with approximately 10 dB of reflection loss at and input frequency of 8 GHz. Many efforts have been made to fabricate the CIP-based polymeric composites for EMI shielding, but few studies have investigated the synergistic effects of CNTs and CIP with respect to the EMI shielding capability. Furthermore, investigations into the effect of magnetization curing on the EMI shielding capability of CIP-based nanocomposites have rarely been reported, and this has great potential to improve performance.

Therefore, this study aims to investigate the synergistic effects of CNT and CIP on EMI shielding capability. First, a facile strategy will be proposed to fabricate nanohybrid particles composed of CNTs and CIP (CNT@CIP) directly in an elastic polymer matrix (polydimethylsiloxane, PDMS). The resulting elastic polymer composites, embedded with CNT@CIP nanohybrid particles, can be used for EMI shielding. The formation of the CNT@CIP nanohybrid particles will be confirmed using various characterization tools such as zeta potential analysis, scanning electron microscopy (SEM), Fourier-transform infrared (FT–IR) spectroscopy, and Raman spectroscopy. Subsequently, the effects of the magnetization curing process and the synergy of the incorporated CNT@CIP nanohybrid particles on the EMI shielding capability of the polymeric composites will be investigated.

2. Experimental section

2.1. Specimen preparation

PDMS and its curing agent, purchased from Dow Corning, were used as the polymeric matrix. Multi-walled CNTs (Hyosung Inc.) 12–40 nm in diameter and 10 μm in length, and CIP (BASF) with particles 4.5–6.0 μm in diameter were utilized as electrically conductive fillers. The detailed specifications of the CNTs and CIP were summarized in the previous study performed by the authors [10]. To improve the dispersion of the CNTs, poly sodium 4-styrenesulfonate (PSS) was added to composites as a dispersant [11,21,24]. The compositions of the specimens are given in Table 1.

The method used to fabricate the CNT@CIP nanohybrid particle-embedded polymeric composites is illustrated in Fig. 1. First, the CNTs and PSS were added to a beaker, followed by 100 ml of isopropyl alcohol (IPA). The solution was hand-mixed for 1 min, then sonicated using ultrasonication (40 kHz, 200 W) for 1 h. Next, PDMS was added to the solution, which was mixed using a magnetic stirrer at 200 rpm and heated to 130 °C for 12 h. The curing agent was added once the IPA solvent had evaporated completely, and the mixture was hand-mixed for 1 min. It was then cured in a mold with and inner diameter of 3 mm, outer diameter of 7 mm, and thickness of 10 mm for use in EMI shielding investigations. As the specimens cured, some samples were exposed to a magnetic field to examine the effect of magnetization on the EMI shielding capability (Fig. 1).

2.2. Experimental methods

The solutions prepared for the zeta potential measurements are summarized in Table 2. The zeta potentials of the solutions were measured using a zeta potential analyzer (ELSZ-2000, Otsukael) to examine the dispersion of the conductive fillers. A field emission scanning electron microscope (FE-SEM,

Table 1 – Composition of the fabricated specimens (wt%).

Specimen Code		PDMS		CNTs	PSS	CIP
		Base	Curing agent			
Group-A	C0P0	100	10	0	0	0
	C0.5P0			0.5	0.5	
	C1P0			1.0	1.0	
	C2P0			2.0	2.0	
	C0P10			0	0	10
	C0P30			0	0	30
	C0P50			0	0	50
Group-B	C0.5P10	100	10	0.5	0.5	10
	C1P10			1.0	2.0	
	C2P10			2.0	2.0	
	C0.5P30			0.5	0.5	30
	C1P30			1.0	2.0	
	C2P30			2.0	2.0	
	C0.5P50			0.5	0.5	50
	C1P50			1.0	2.0	
	C2P50			2.0	2.0	

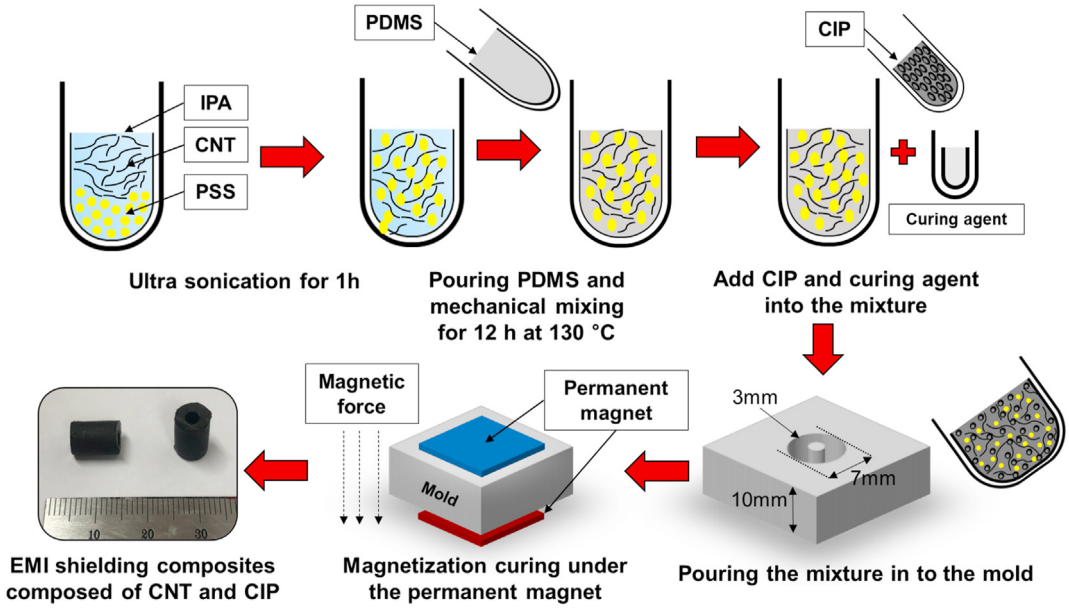

Fig. 1 – Fabrication of CNT@CIP nanohybrid particle-embedded polymeric composites.

Hitachi S4800) was used to obtain microstructural images showing the formation of the nanohybrid particles composed of CNTs and CIP. The SEM images were discussed with respect to their corresponding zeta potentials. The FT-IR spectra of the CNTs, CIP, and CNT@CNT nanohybrid particles were examined using a FTIR-7600 (Lambda scientific, Australia). The Raman spectra of the CNTs and CNT@CIP nanohybrid particles were obtained using a XperRam S (Nanobase Inc., South Korea). The electrical resistances of the fabricated specimens were measured using a portable multi-meter (U1281A, Keysight Technologies) with the two-probe method. The electrical resistance was used to calculate the electrical resistivity and electrical conductivity using the equation [25–27].

$$\sigma = \rho^{-1} = L \times A^{-1} \times R^{-1} \quad (1)$$

where σ and ρ denote the electrical conductivity and resistivity, respectively; and L, A, and R indicate the length, area, and measured electrical resistance of the specimens, respectively [21]. The EMI shielding capability of the specimens, expressed as the shielding effectiveness, was measured using a programmable network analyzer (PNA; N5239A, Agilent Technologies) and 7-mm airline instrument (85050D, Agilent Technologies) at frequencies between 300 MHz and 8.5 GHz [28], as shown in Fig. 2. An EM wave was generated at port 1 and flowed to port 2. The intensity of the EM wave at port i and port j was measured using the network analyzer, and the difference between the readings was expressed as S_{ij}. Thus, the intensity of the incidence, reflection, and transmission waves was obtained, as the reflection and absorption losses were given by S_{11} and S_{12}, respectively [29] (Fig. 2b).

Table 2 – Composition of the solutions used for zeta potential analysis.

Solution	IPA (mL)	CNTs (g)	CIP (g)
IPA with CNTs	40	0.01	0
IPA with CIP	40	0	0.2
IPA with CNTs and CIP	40	0.01	0.2

3. Results and discussion

The zeta potentials of the solutions containing IPA, IPA with CNTs, IPA with CIP, and IPA with CNTs and CIP are summarized in Table 3. The relative surface charges of the CNTs and CIP were positive (5.94 eV) and negative (−28.2 eV), respectively. These opposing surface charges indicate that the CNTs and CIP can be hybridized through electrostatic interaction [30]. This hypothesis was verified by the intermediate surface charge of the CNT@CIP nanohybrid particles (−2.89 eV).

SEM images showed that the CNTs were approximately 15–40 nm long and 100 μm in diameter (Fig. 3a), and that the CIP particles had a broad size distribution with diameters between 300 nm and 5 μm (Fig. 3b). As expected, SEM images of the CNT@CIP nanohybrid particles confirmed that individual CNTs were attached to the surfaces of the CIP (Fig. 3c) [31]. This agrees with the results of the zeta potential analysis (Table 3).

The FT-IR spectrum for the CNTs showed peaks at 1095 cm^{-1} from typical of C-O stretching, 1214 cm^{-1} from C-O-C stretching, 1382 cm^{-1} from O-H deformation, 1631 cm^{-1} from aromatic C=C stretching, 1735 cm^{-1} from C=O stretching, and 3451 cm^{-1} from O-H stretching, respectively (Fig. 3d) [32]. The FT-IR spectrum for CIP was almost featureless, but there were peaks at 1382, 1627, and 3451 cm^{-1} from O-H deformation, C=O carbonyl stretching, and O-H stretching, respectively. The FT-IR spectra for the CNTs and CIP suggested that their surfaces were decorated with a few oxygen-containing functional groups, thus they could form hydrogen bonds (Fig. 3d). As expected, the

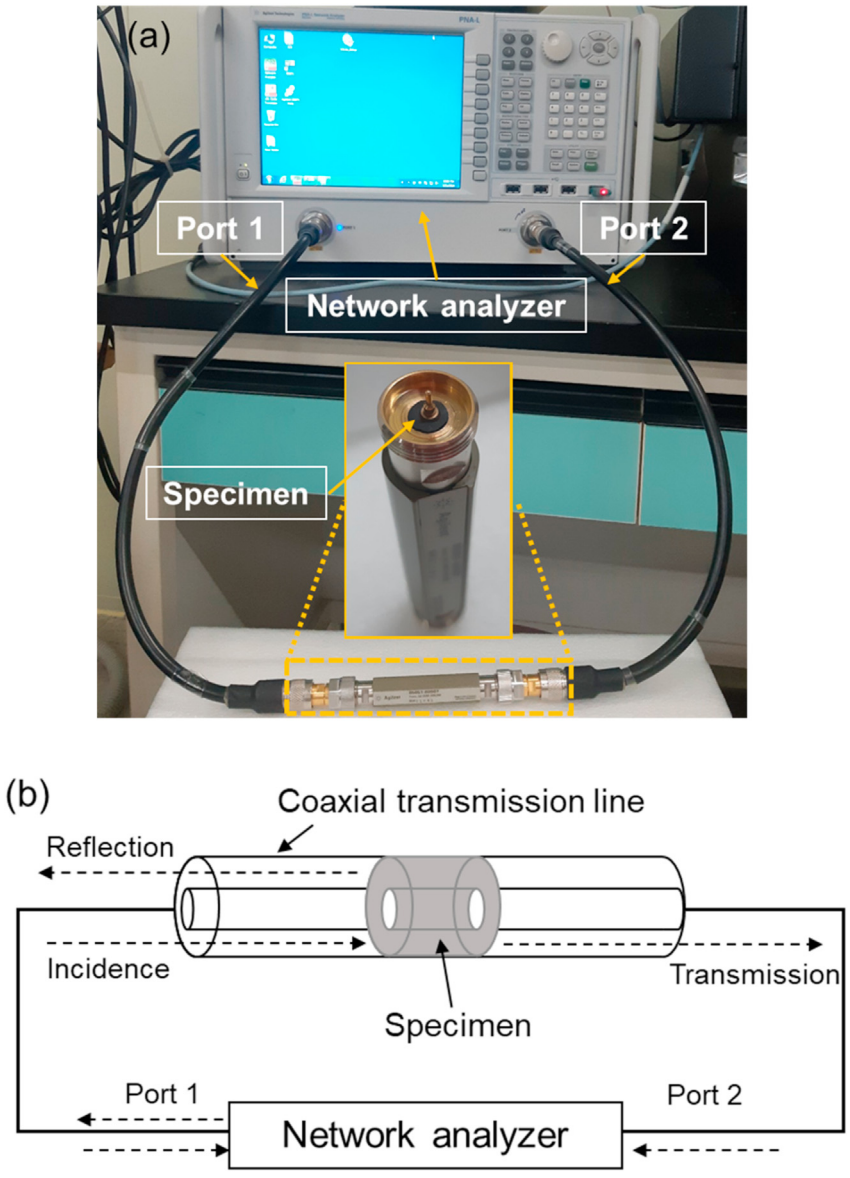

Fig. 2 – (a) Experimental setup used to measure EMI shielding effectiveness, and (b) principle of PNA.

FT-IR spectrum for the CNT@CIP nanohybrid particles showed a superposition of the features of the CNTs and CIP.

The Raman spectrum for the CNTs exhibited characteristic D- and G-peaks at 1337 and 1594 cm^{-1}, which originate from the disordered and ordered sp^2 carbon domains, respectively (Fig. 3e) [33]. After hybridization with CIP, the D- and G-peaks were shifted to 1341 and 1600 cm^{-1}, respectively. There was also a slight decrease in the relative intensity of the D- and G-peaks (I_D/I_G), from 1.20 ± 0.04 to 1.17 ± 0.06 (Fig. 3e), which is an indicator of crystallinity in graphitic carbon materials [33]. All the spectroscopic analyses indicated that the CNTs and CIP were well hybridized with strongly-interactive interfaces. It should be noted that the incorporation of CNT@CIP nanohybrid particles into PDMS matrix did not lead to the changes of their I_D/I_G value (Fig. 3f).

The electrical resistivity and conductivity of the fabricated specimens are shown in Fig. 4. The electrical conductivity increased dramatically from 4.05×10^{-9} to 1.02×10^{-5} S/cm as the CNT content increased from 0.5 to 1.0 wt% (Fig. 4). This range indicated a percolation threshold, meaning the electrical conductivity increased by three orders of magnitude as the CNT content increased [34–36]. The observed percolation

Table 3 – Zeta potential values of the CNTs and CIP in IPA solution.

Zeta potential value (mV)	IPA	IPA with CNTs	IPA with CIP	IPA with CNTs and CIP
Absolute values	−15.71	−9.77	−43.91	−18.60
Relative values	0	5.94	−28.20	−2.89

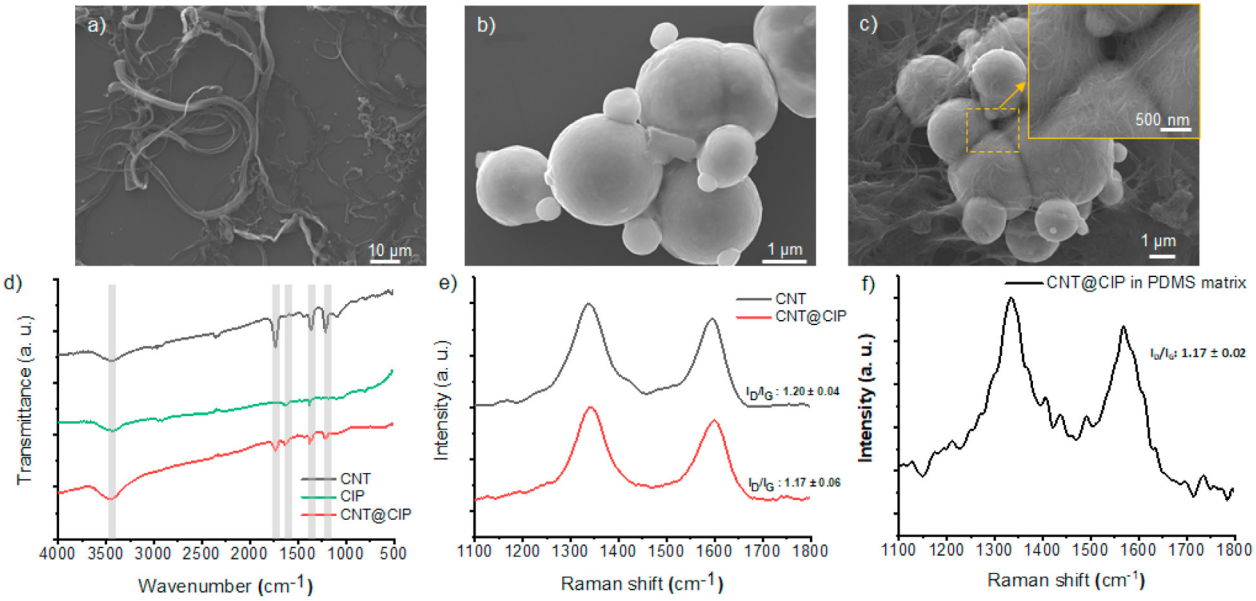

Fig. 3 – SEM images of (a) CNTs, (b) CIP, and (c) CNT@CIP nanohybrid particles. (d) FT-IR spectra of CNTs, CIP, and CNT@CIP nanohybrid particles. (e) Raman spectra of CNTs and CNT@CIP nanohybrid particles. (f) Raman spectra of CNT@CIP incorporated PDMS.

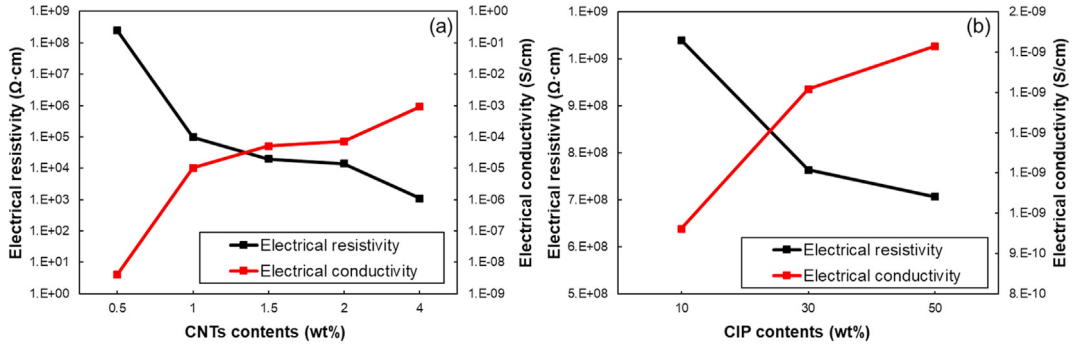

Fig. 4 – Electrical resistivity and conductivity of specimens with different (a) CNT and (b) CIP contents.

threshold was equal to or less than those reported in previous studies [21,34]. Furthermore, the electrical conductivity increased as the embedded CIP content increased from 9.61×10^{-10} to 1.41×10^{-9} S/cm (Fig. 4b); however, CIP inclusion had a much smaller effect on the electrical conductivity than the CNTs.

The effect of the CNT and CIP contents on the shielding effectiveness of the specimens is illustrated in Fig. 5. The EMI shielding effectiveness increased as the CNT and CIP contents increased. The specimens without CIP and with CNT contents of 0%, 0.5%, 1%, and 2% showed shielding effectiveness of approximately −0.52, −5.64, −10.92, and −16.54 dB, respectively, at 8.9 GHz (Fig. 5a). In addition, the specimens without CNTs and with CIP contents of 0%, 10%, 30%, and 50% showed shielding effectiveness of approximately −0.52, −0.81, −1.96, and −3.23 dB, respectively, at 8.9 GHz (Fig. 5b). From this, it can be concluded that the addition of CNTs has a greater effect on EMI shielding effectiveness than the addition of CIP. This can be explained by the fact that EMI shielding effectiveness is proportional to electrical conductivity [18,37,38]. Thus, the EMI shielding effectiveness results showed good agreement with the measured electrical conductivity shown in Fig. 4 and previous studies [18,37,38].

The effects of magnetization curing on the electrical conductivity of the specimens with various CNT and CIP contents were investigated. The electrical conductivities of C0.5P10, C1P10, and C2P10 were 1.84×10^{-8}, 2.09×10^{-7}, and 3.15×10^{-7} S/cm, respectively. These values were not significantly affected by an increase in the CIP content to 30% or 50% after conventional curing (Fig. 6). In contrast, the electrical conductivities of the specimens increased to 3.18×10^{-8}, 5.96×10^{-7}, and 2.26×10^{-6} S/cm, respectively, when they were cured under magnetization (Fig. 6). These results indicate that magnetization curing improved the electrical conductivity of the specimens. In particular, the electrical conductivity of the specimens with 0.5% and 1% CNT were not significantly affected when the CIP content was increased to 30%, despite magnetization curing. However, the electrical conductivity increased significantly to 7.18×10^{-8} and 9.91×10^{-7} S/cm, respectively, with magnetization curing when the CIP content was 50% (Fig. 6a, b). It is noteworthy that the electrical conductivity of the C2P10 specimens linearly

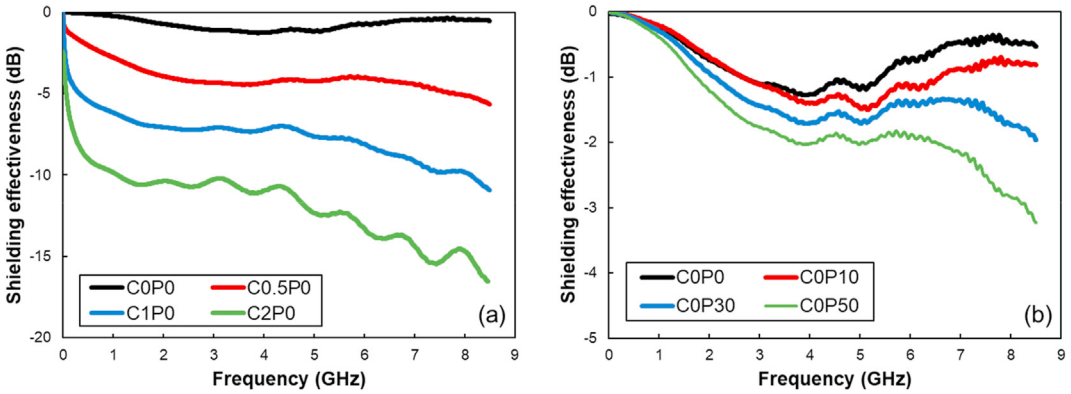

Fig. 5 – EMI shielding effectiveness of specimens with different (a) CNT and (b) CIP contents.

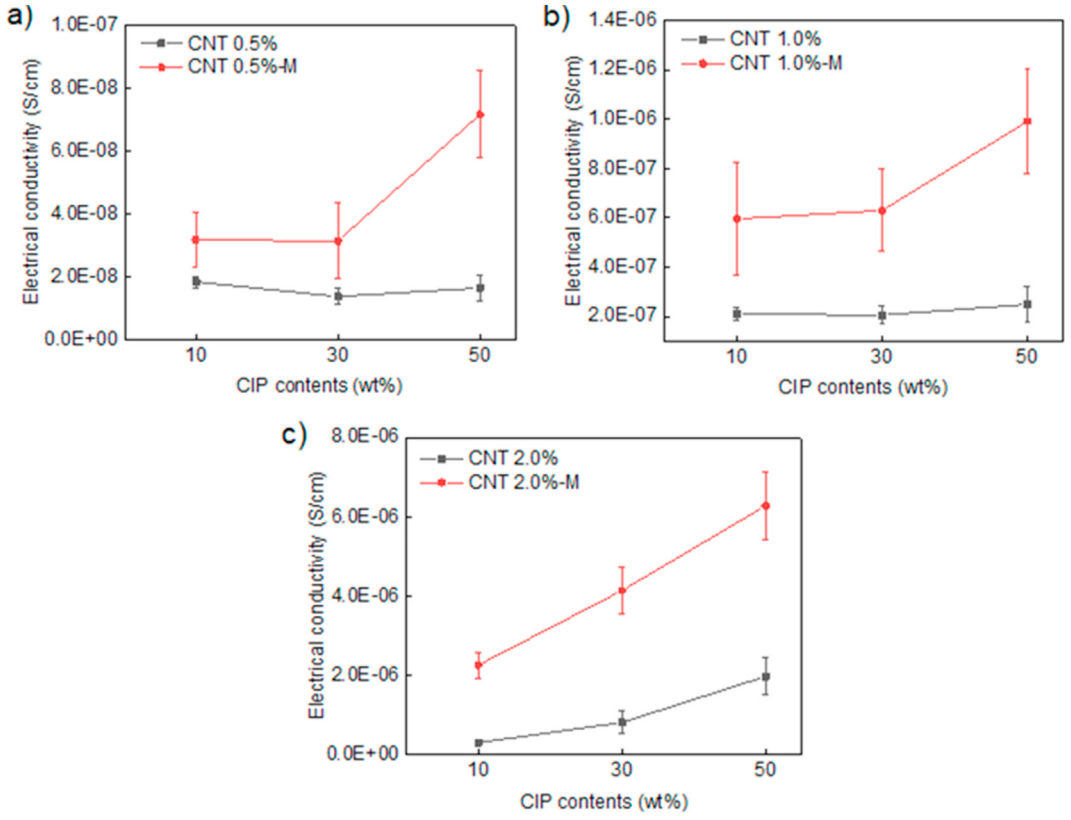

Fig. 6 – Electrical conductivity of specimens with (a) 0.5%, (b) 1.0%, and (c) 2.0% CNT content, and 10%, 30%, and 50% CIP content under conventional and magnetization curing.

increased to 4.14×10^{-6} and 6.28×10^{-6} S/cm under magnetization curing when the CIP content was 30% and 50%, respectively (Fig. 6c). These results clearly indicate that magnetization curing enhanced the electrical conductivity of the specimens. According to the previous studies, it has been reported that the hybridization of natural filler with the addition of nano-sized CNTs can mitigate the weak interfacial bonding between CNT and polymer matrix, improving the mechanical properties of the composites [39,40]. Thus, based on the findings derived from this study, it can be said that the utilization of CIP and magnetization curing may improve both mechanical and electrical properties of the fabricated composites.

The interesting changes in the electrical conductivity of the specimens can be attributed to the alignment of the CNT@CIP nanohybrid particles during the magnetization curing process. As reported previously, individual CNTs can wrap the CIP particles when the CNTs and CIP are combined in polymeric composites [10]. The CIP-based polymeric composites respond to the magnetic field, leading to the formation of CIP-based chain-like structures (Fig. 7) [41–43]. Thus, the CNT@CIP nanohybrid particles can efficiently form dense electrically conductive networks in the polymeric matrix through the alignment of these structures, improving the electrical conductivity (Fig. 7a, b, c). As a control, a C2P50 specimen was fabricated without magnetization curing, and the aligned

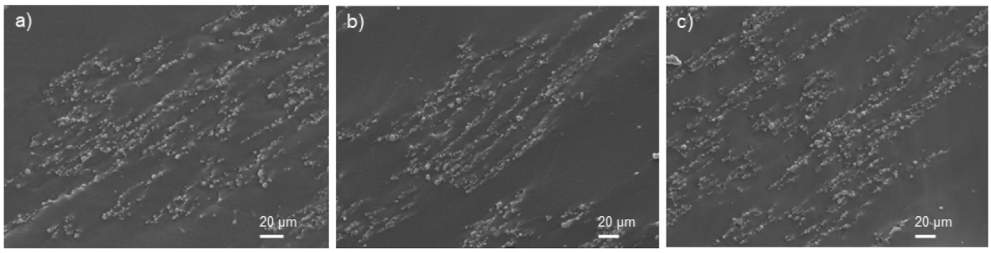

Fig. 7 – SEM images of specimens prepared with (a) 10%, (b) 30%, and (c) 50% CIP content, without CNT, and with magnetization curing.

structures did not form (Fig. 8d). This control specimen clearly showed the importance of magnetization curing in the construction of aligned chain-like structures of CNT@CIP nanohybrid particles.

The effect of magnetization curing on EMI shielding effectiveness was explored. Figure 9 shows that the EMI shielding effectiveness with and without magnetization curing was −5.82 and −5.78 dB, respectively, for specimen C0.5P10, and -12.58 and −14.33 dB, respectively, for specimen C0.5P10. These results indicate that EMI shielding effectiveness was not affected by magnetization curing (Fig. 9a). In contrast, the EMI shielding effectiveness of C2P10 specimen was greatly enhanced by magnetization curing. The EMI shielding effectiveness of C2P10 specimens fabricated with and without magnetization curing were −14.55 and −19.51 dB, respectively. This indicates that the CNT content is an important factor in the creation of electrically conductive networks (Fig. 9a). Moreover, the EMI shielding effectiveness increased as the CIP content increased. The EMI shielding effectiveness of C0.5P30, C1P30, and C2P30 specimens was commonly enhanced by magnetization curing (Fig. 9b), and the degree of this enhancement was further augmented by increasing CIP content to 50% (Fig. 9c). Thus, it is clear that magnetization curing can significantly improve the EMI shielding effectiveness of polymeric composites containing CNT@CIP nanohybrid particles. This phenomena can be attributed to the formation of a percolation network of aligned CNT@CIP nanohybrid particles in the polymeric matrix during the magnetization curing process (Fig. 8a, b, c).

The EMI shielding capability of the specimens observed in the present study is compared with that found in the similar literatures [6,12,44]. Lei et al. developed Au@CNT-incorporated PDMS composites, and it showed about 10 dB of shielding capability at 8 GHz [6]. The CNT-embedded polymeric

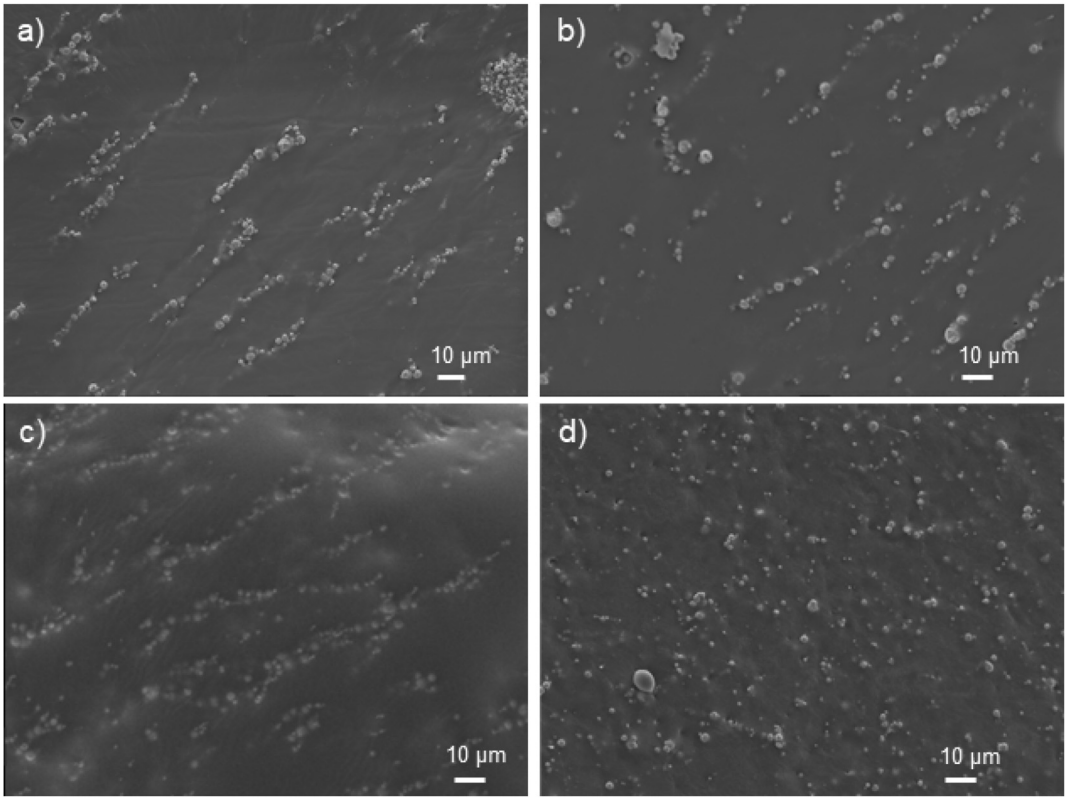

Fig. 8 – SEM images of specimens (a) C0.5P50-M, (b) C1P50-M, and (c) C2P50-M fabricated using magnetization curing. (d) SEM image of specimen C2P50 fabricated without magnetization curing.

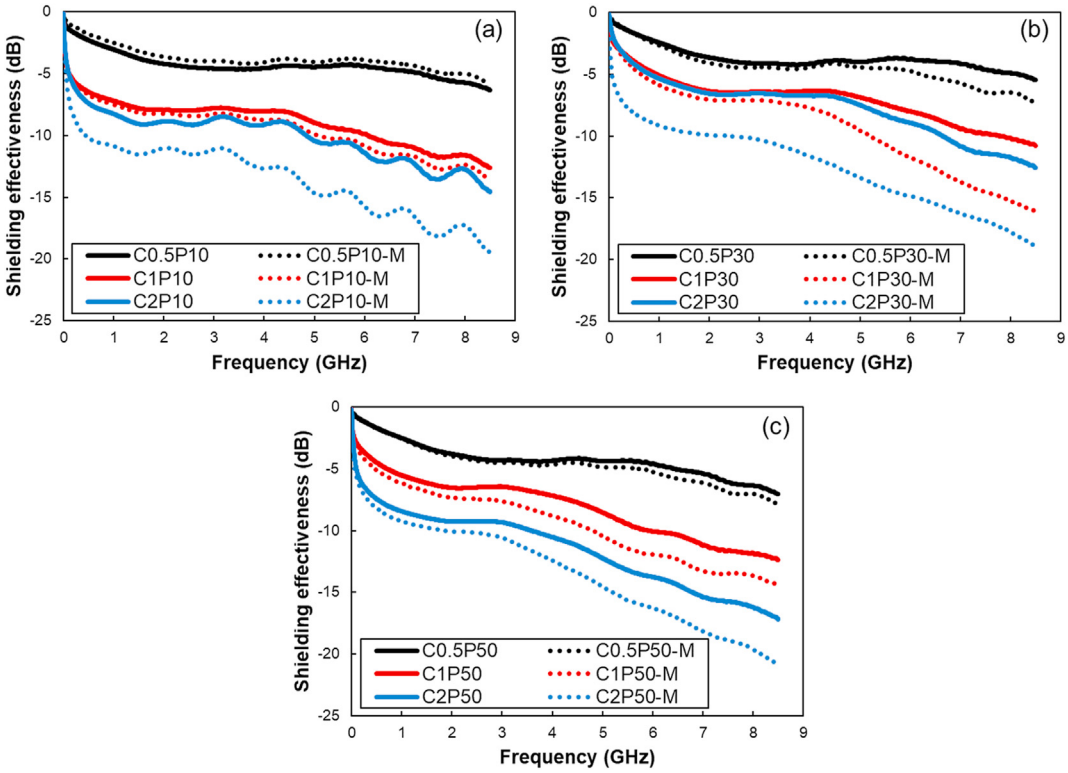

Fig. 9 – Effect of magnetization curing on the EMI shielding effectiveness of the specimens with (a) CIP 10%, (b) CIP 30%, and (C) CIP 50%.

composites fabricated in Wang et al. exhibited approximately 12 and 18 dB of shielding effectiveness at 8.2 GHz, when 1 and 2 wt.% of CNT was added to the composites [12]. These values are lower than that found in the present study, indicating 15 and 20 dB of shielding effectiveness when 1 and 2 wt.% of CNT was used (Fig. 9). In addition, Al-Saleh et al. manufactured CNT-embedded PP/PE blended polymeric composites, and it showed approximately 18 db of EMI shielding capability when both CNT 5.1 wt.% and GNP 4.4% were added to the composites [44]. This EMI shielding capability can be obtained in the present study by using only less than 2 wt.% of CNT was used (Fig. 9). In this regard, it can be said that the fabricated polymeric composites using the proposed CNT@CIP nanohybrid particles showed enhanced EMI shielding performances with low amount of fillers.

Figure 10 represents the mechanism analyses of developing CNT@CIP nanohybrid particles and the magnetization curing method. The CIP was utilized to allow individual CNT particles to adhere to the CIP surface since the CIP can be easily controlled by the magnetic force (Fig. 10a). The CNT@CIP nanohybrid particles were then embedded into the polymeric composites for fabricating the conductive polymeric composites. During the curing process, the magnetic force was applied to the specimens for aligning the CNT@CIP nanohybrid particles in a specific direction (Fig. 10b). As the CNT@CIP nanohybrid particles aligned in a direction, the extent of forming conductive networks increased, improving the electrical conductivity of the specimens. The total EMI shielding capability (SE_{total}) of the conductive polymeric composites can be calculated by following equation [45]:

$$SE_{total} = 39.5 + 10\log\frac{\sigma}{2\pi f\mu} + 8.7\sqrt{\pi f\mu\sigma} \quad (2)$$

where μ and d denote the permeability and thickness of the specimens, respectively.

Meanwhile, the previous studies reported that the interfacial bonding between the conductive fillers and polymer matrix is possibly increased with increasing of the effective contact area [46,47]. As found in the present study, the development of CNT@CIP nanohybrid particles can lead to the increase of contact area with the polymer matrix compared to that found when only CNT or CIP particles are added in the polymer matrix. In addition, it has been reported that the increased interfacial bonding caused by the increasing contact area can improve the connection of conductive fillers in the polymer matrix, which are in close agreement with the results in the present study [46,47]. For these reasons, it can be said that the utilization of CNT@CIP nanohybrid particles can increase both effective contact area and interfacial bonding, thereby leading to the improvement on electrical conductivity of the polymeric composites.

In this regard, the proposed methods including development of CNT@CIP nanohybrid particles and magnetization curing method can reduce the CNT content required to obtain a given electrical conductivity and EMI shielding capability, demonstrating the potential of reducing fabrication costs. In addition, the present method is expected to be used in

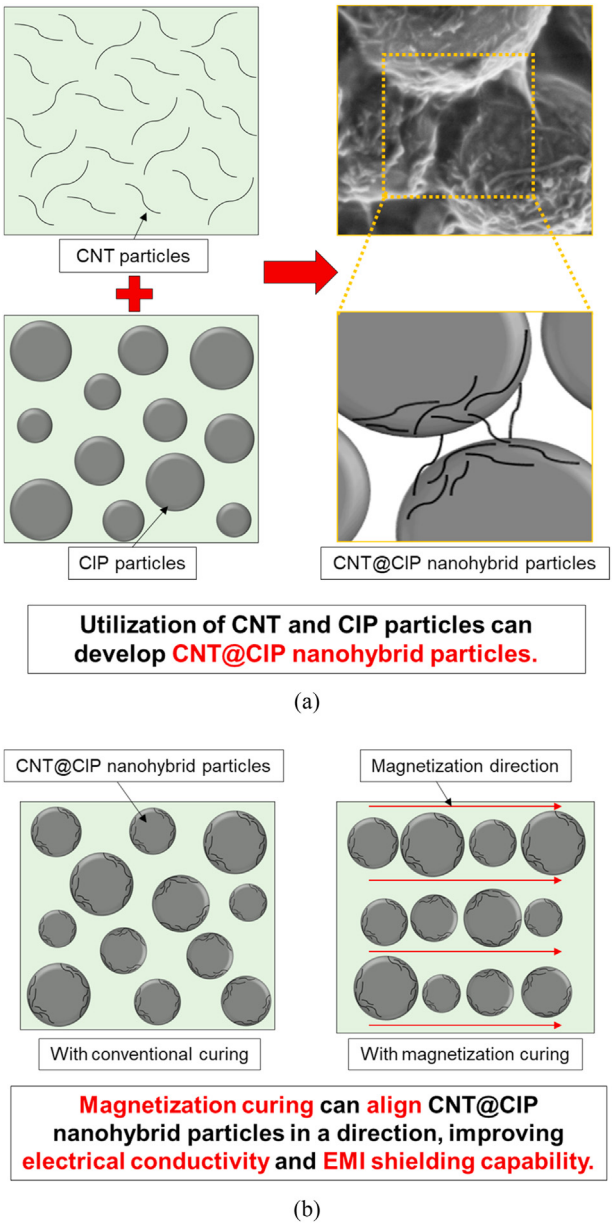

Fig. 10 – Mechanism analyses of (a) developing CNT@CIP nanohybrid particles, and (b) advantages of magnetization curing method.

fabricating conductive polymeric composites with high electrical conductivity for various functional purposes such as piezoresistive sensors and/or electrical heating composites.

4. Conclusion

This study proposed a novel method for manufacturing electrically conductive fillers composed of CNT@CIP nanohybrid particles-embedded polymeric composites, and investigated their electrical conductivity and EMI shielding capability. The CNT@CIP nanohybrid particles were prepared by attaching CNT particles to the surface of CIP through an electrostatic interaction. The interfacing structure of the CNT@CIP nanohybrid particles was systematically characterized using various tools, showing that they have strongly interactive interfaces.

Conductive polymeric composites were fabricated successfully by incorporating the CNT@CIP nanohybrid particles into an elastic polymer matrix. The effects of magnetization curing on the electrical conductivity and EMI shielding capability of the polymeric composites were examined with respect to the alignment of the CNT@CIP nanohybrid particles. The magnetization curing process aligned the CNT@CIP nanohybrid particles into chain-like structures, which considerably improved the electrical conductivity and EMI shielding capability of the composites compared to those fabricated without magnetization curing. The CNT@CIP nanohybrid particles-embedded polymeric composites fabricated with magnetization curing have great potential for use as EMI shielding composites across various practical applications.

Authorship contribution statement

Daeik Jang: Writing–original draft, Conceptualization, Investigation, Visualization. **H.N. Yoon:** Investigation, Visualization. **Joonho Seo:** Formal analysis, Writing-Reviewing and Editing. **Hyun Jun Cho:** Investigation, Visualization. **G. M. Kim:** Formal analysis. **Young-Kwan Kim:** Formal analysis, Writing - review & editing, Supervision. **Beomjoo Yang:** Writing - review & editing, Supervision, Resources.

Declaration of Competing Interest

The authors declare that they have no known competing financial interests or personal relationships that could appear to have influenced the work reported in this paper.

Acknowledgments

This study was supported by a grant from the National Research Foundation of Korea (NRF) funded by the Korea government (MSIT) (2020R1C1C1005063 and No. 2020R1F1A1070831) and was supported and funded by the Korean National Police Agency [Project Name: Development of onsite support equipment for criminal safety arrest/Project Number: PR08-01-000-20]. In addition, this study was supported by the Basic Research Project of the Korea Institute of Geoscience and Mineral resources (KIGAM) funded by the Ministry of Science and ICT of Korea (GP2022-002).

REFERENCES

[1] Yoon HN, Jang D, Lee HK, Nam IW. Influence of carbon fiber additions on the electromagnetic wave shielding characteristics of CNT-cement composites. Construct Build

Mater 2020;269:121238. https://doi.org/10.1016/j.conbuildmat.2020.121238.
[2] Zhong L, Yu R, Hong X. Review of carbon-based electromagnetic shielding materials: film, composite, foam, textile. Textil Res J 2021;91:1167–83. https://doi.org/10.1177/0040517520968282.
[3] Jia Z, Kou K, Yin S, Feng A, Zhang C, Liu X, et al. Magnetic Fe nanoparticle to decorate N dotted C as an exceptionally absorption-dominate electromagnetic shielding material. Compos B Eng 2020;189:107895. https://doi.org/10.1016/j.compositesb.2020.107895.
[4] Zhang W, Zhao H, Hu X, Ju D. A novel processing for CNT-reinforced Mg-matrix laminated composites to enhance the electromagnetic shielding property. Coatings 2021:1–10.
[5] Zhao X, Xu L, Chen Q, Peng Q, Yang M, Zhao W, et al. Highly conductive multifunctional rGO/CNT hybrid sponge for electromagnetic wave shielding and strain sensor. Adv Mater Technol 2019;4:1–9. https://doi.org/10.1002/admt.201900443.
[6] Lei X, Zhang X, Song A, Gong S, Wang Y, Luo L, et al. Investigation of electrical conductivity and electromagnetic interference shielding performance of Au@CNT/sodium alginate/polydimethylsiloxane flexible composite. Compos Part A Appl Sci Manuf 2020;130:105762. https://doi.org/10.1016/j.compositesa.2019.105762.
[7] Yang B, Kim G, Resources M. Effect of CNT agglomeration on the electrical conductivity and percolation threshold of nanocomposites : a micromechanics- based approach. 2014.
[8] Iqbal A, Sambyal P, Koo CM. 2D MXenes for electromagnetic shielding: a review. Adv Funct Mater 2020;30:1–25. https://doi.org/10.1002/adfm.202000883.
[9] Jang D, Choi BH, Yoon HN, Yang B, Lee HK. Improved electromagnetic wave shielding capability of carbonyl iron powder-embedded lightweight CFRP composites. Compos Struct 2022;286:115326. https://doi.org/10.1016/j.compstruct.2022.115326.
[10] Jang D, Farooq SZ, Yoon HN, Khalid HR. Design of a highly flexible and sensitive multi-functional polymeric sensor incorporating CNTs and carbonyl iron powder. Compos Sci Technol 2021;207:108725. https://doi.org/10.1016/j.compscitech.2021.108725.
[11] Jang D, Kil T, Yoon HN, Seo J, Khalid HR. Artificial neural network approach for predicting tunneling-induced and frequency-dependent electrical impedances of conductive polymeric composites. Mater Lett 2021;302:130420. https://doi.org/10.1016/j.matlet.2021.130420.
[12] Wang H, Zhu D, Zhou W, Luo F. Effect of multiwalled carbon nanotubes on the electromagnetic interference shielding properties of polyimide/carbonyl iron composites. Ind Eng Chem Res 2015;54:6589–95. https://doi.org/10.1021/acs.iecr.5b01182.
[13] Bhandari Manan, Wang Jianchao, Jang Daeik, IlWoo Nam BH. A comparative study on the electrical and piezoresistive sensing characteristics of GFRP and CFRP composites with hybridized incorporation of carbon nanotubes, graphenes, carbon nanofibers, and graphite nanoplatelets. Sensors 2021;21:7291.
[14] Jang D, Yoon HN, Seo J, Park S, Kil T, Lee HK. Improved electric heating characteristics of CNT-embedded polymeric composites with an addition of silica aerogel. Compos Sci Technol 2021;212:108866. https://doi.org/10.1016/j.compscitech.2021.108866.
[15] Kato Y, Horibe M, Ata S, Yamada T, Hata K. Stretchable electromagnetic-interference shielding materials made of a long single-walled carbon-nanotube-elastomer composite. RSC Adv 2017;7:10841–7. https://doi.org/10.1039/c6ra25350d.
[16] Jang D, Park J-E, Kim Y-K. Evaluation of (CNT@CIP)-Embedded magneto-resistive sensor based on carbon nanotube and carbonyl iron powder polymer composites. Polymers 2022;14:542. https://doi.org/10.2307/j.ctvcm4g8n.8.
[17] Nam IW, Lee HK, Jang JH. Electromagnetic interference shielding/absorbing characteristics of CNT-embedded epoxy composites. Compos Part A Appl Sci Manuf 2011;42:1110–8. https://doi.org/10.1016/j.compositesa.2011.04.016.
[18] Chen Y, Zhang H Bin, Huang Y, Jiang Y, Zheng WG, Yu ZZ. Magnetic and electrically conductive epoxy/graphene/carbonyl iron nanocomposites for efficient electromagnetic interference shielding. Compos Sci Technol 2015;118:178–85. https://doi.org/10.1016/j.compscitech.2015.08.023.
[19] Wang LR, Yu M, Yang PA, Qi S, Fu J. Synthesis of absorbing coating based on magnetorheological gel with controllable electromagnetic wave absorption properties. Smart Mater Struct 2019;28. https://doi.org/10.1088/1361-665X/ab06e8.
[20] Sedlacik M, Mrlik M, Babayan V, Pavlinek V. Magnetorheological elastomers with efficient electromagnetic shielding. Compos Struct 2016;135:199–204. https://doi.org/10.1016/j.compstruct.2015.09.037.
[21] Jang DI, Yoon HN, Nam IW, Lee HK. Effect of carbonyl iron powder incorporation on the piezoresistive sensing characteristics of CNT-based polymeric sensor. Compos Struct 2020;244:112260. https://doi.org/10.1016/j.compstruct.2020.112260.
[22] Jang DI, Yun GE, Park JE, Kim YK. Designing an attachable and power-efficient all-in-one module of a tunable vibration absorber based on magnetorheological elastomer. Smart Mater Struct 2018;27:85009. https://doi.org/10.1088/1361-665X/aacdbd.
[23] Park J-E, Yun G-E, Jang D-I, Kim Y-K. Analysis of electrical resistance and impedance change of magnetorheological gels with DC and AC voltage for magnetometer application. Sensors 2019;19:2510. https://doi.org/10.3390/s19112510.
[24] Jang D, Yoon HN, Seo J, Yang B. Effects of exposure temperature on the piezoresistive sensing performances of MWCNT-embedded cementitious sensor. J Build Eng 2022;47:103816. https://doi.org/10.1016/j.jobe.2021.103816.
[25] Jang D, Yoon HN, Farooq SZ, Lee HK, Nam IW. Influence of water ingress on the electrical properties and electromechanical sensing capabilities of CNT/cement composites. J Build Eng 2021;42:103065. https://doi.org/10.1016/j.jobe.2021.103065.
[26] Jang D, Yoon HN, Seo J, Lee HK, Kim GM. Effects of silica aerogel inclusion on the stability of heat generation and heat-dependent electrical characteristics of cementitious composites with CNT. Cement Concr Compos 2021;115:103861. https://doi.org/10.1016/j.cemconcomp.2020.103861.
[27] Jang D, Yoon HN, Seo J, Park S. Enhanced electrical heating capability of CNT-embedded cementitious composites exposed to water ingress with addition of silica aerogel. Ceram Int 2022. https://doi.org/10.1016/j.ceramint.2022.01.216.
[28] Nam IW, Lee HK. Synergistic effect of MWNT/fly ash incorporation on the EMI shielding/absorbing characteristics of cementitious materials. Construct Build Mater 2016;115:651–61. https://doi.org/10.1016/j.conbuildmat.2016.04.082.
[29] Al-Saleh MH, Sundararaj U. Electromagnetic interference shielding mechanisms of CNT/polymer composites. Carbon N Y 2009;47:1738–46. https://doi.org/10.1016/j.carbon.2009.02.030.
[30] Kim GM, Kil T, Lee HK. A novel physicomechanical approach to dispersion of carbon nanotubes in polypropylene composites. Compos Struct 2020;258:113377. https://doi.org/10.1016/j.compstruct.2020.113377.
[31] Park HM, Park C, Bang J, Lee M, Yang B. Synergistic effect of MWCNT and carbon fiber hybrid fillers on electrical and

mechanical properties of alkali-activated slag composites. Crystals 2020;10:1–10. https://doi.org/10.3390/cryst10121139.
[32] Jeon J, Choi M, Kim SB, Seo TH, Ku BC, Ryu S, et al. Eggshell membrane hydrolysate as a multi-functional agent for synthesis of functionalized graphene analogue and its catalytic nanocomposites. J Ind Eng Chem 2021;102:233–40. https://doi.org/10.1016/j.jiec.2021.07.010.
[33] Yoon CJ, Lee SH, Kwon Y Bin, Kim K, Lee KH, Kim SM, et al. Fabrication of sustainable and multifunctional TiO2@carbon nanotube nanocomposite fibers. Appl Surf Sci 2021;541:148332. https://doi.org/10.1016/j.apsusc.2020.148332.
[34] Bauhofer W, Kovacs JZ. A review and analysis of electrical percolation in carbon nanotube polymer composites. Compos Sci Technol 2009;69:1486–98. https://doi.org/10.1016/j.compscitech.2008.06.018.
[35] Khalid HR, Choudhry I, Jang D, Abbas N, Haider MS, Lee HK. Facile synthesis of sprayed CNTs layer-embedded stretchable sensors with controllable sensitivity. Polymers 2021;13:1–6.
[36] Jang HG, Yang B, Khil MS, Kim SY, Kim J. Comprehensive study of effects of filler length on mechanical, electrical, and thermal properties of multi-walled carbon nanotube/polyamide 6 composites. Compos Part A Appl Sci Manuf 2019;125:105542. https://doi.org/10.1016/j.compositesa.2019.105542.
[37] Shukla V. Review of electromagnetic interference shielding materials fabricated by iron ingredients. Nanoscale Adv 2019;1:1640–71. https://doi.org/10.1039/c9na00108e.
[38] Yang Y, Zuo Y, Feng L, Hou X, Suo G, Ye X, et al. Powerful and lightweight electromagnetic-shielding carbon nanotube/graphene foam/silicon carbide composites. Mater Lett 2019;256:126634. https://doi.org/10.1016/j.matlet.2019.126634.
[39] Prabhudass JM, Palanikumar K, Natarajan E, Markandan K. Enhanced thermal stability, mechanical properties and structural integrity of MWCNT filled bamboo/kenaf hybrid polymer nanocomposites. Materials 2022;15. https://doi.org/10.3390/ma15020506.
[40] Shirvanimoghaddam K, Abolhasani MM, Polisetti B, Naebe M. Periodical patterning of a fully tailored nanocarbon on CNT for fabrication of thermoplastic composites. Compos Part A Appl Sci Manuf 2018;107:304–14. https://doi.org/10.1016/j.compositesa.2018.01.015.
[41] Kim Y-K, Kim J, Jang D, Kim S, Jung W. A study on the effects of multiwall carbon nanotubes on dynamic stiffness of hydrophilic-base magnetorheological gel. Curr Nanosci 2018;15:319–23. https://doi.org/10.2174/1573413714666181023144334.
[42] Kim S, Kim P, Park CY, Choi SB. A new tactile device using magneto-rheological sponge cells for medical applications: experimental investigation. Sensors Actuators, A Phys 2016;239:61–9. https://doi.org/10.1016/j.sna.2016.01.016.
[43] Yu M, Yang P, Fu J, Liu S, Choi SB. A theoretical model for the field-dependent conductivity of magneto-rheological gels and experimental verification. Sensors Actuators, A Phys 2016;245:127–34. https://doi.org/10.1016/j.sna.2016.05.008.
[44] Al-Saleh MH. Electrical, EMI shielding and tensile properties of PP/PE blends filled with GNP:CNT hybrid nanofiller. Synth Met 2016;217:322–30. https://doi.org/10.1016/j.synthmet.2016.04.023.
[45] Kong L, Yin X, Xu H, Yuan X, Wang T, Xu Z, et al. Powerful absorbing and lightweight electromagnetic shielding CNTs/RGO composite. Carbon N Y 2019;145:61–6. https://doi.org/10.1016/j.carbon.2019.01.009.
[46] Yan F, Liu L, Li M, Zhang M, Shang L, Xiao L, et al. One-step electrodeposition of Cu/CNT/CF multiscale reinforcement with substantially improved thermal/electrical conductivity and interfacial properties of epoxy composites. Compos Part A Appl Sci Manuf 2019;125:105530. https://doi.org/10.1016/j.compositesa.2019.105530.
[47] Chen J, Yan L, Song W, Xu D. Interfacial characteristics of carbon nanotube-polymer composites: a review. Compos Part A Appl Sci Manuf 2018;114:149–69. https://doi.org/10.1016/j.compositesa.2018.08.021.